AD-A049 209 AERONAUTICAL RESEARCH LABS MELBOURNE (AUSTRALIA) F/G 11/6
THE DEVELOPMENT OF DRAWING TEXTURES IN COPPER,(U)
JUL 77 R A COYLE, R B NETHERCOTT
UNCLASSIFIED ARL/MAT. 105 NL

| OF |
AD
A049 209

END
DATE
FILMED
2-78
DDC

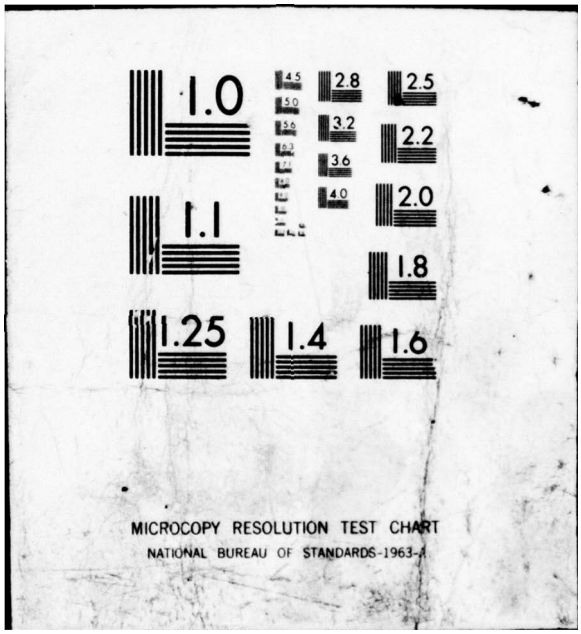
1.0
1.1
1.25
1.4
1.6
1.8
2.0
2.2
2.5
2.8
3.2
3.6
4.0
4.5
5.0
5.6
MICROCOPY RESOLUTION TEST CHART
NATIONAL BUREAU OF STANDARDS-1963-A

ARL / Mat. Report 105

AR - 000 - 736

DEPARTMENT OF DEFENCE

DEFENCE SCIENCE AND TECHNOLOGY ORGANISATION

AERONAUTICAL RESEARCH LABORATORIES

MELBOURNE, VICTORIA

MATERIALS REPORT 105

THE DEVELOPMENT OF DRAWING TEXTURES IN COPPER

R. A. COYLE and R. B. NETHERCOTT

COPY No 12

JULY 1977

AR-000-736

DEPARTMENT OF DEFENCE

DEFENCE SCIENCE AND TECHNOLOGY ORGANISATION

AERONAUTICAL RESEARCH LABORATORIES

(14) ARL/MAT.R105

MATERIALS REPORT 105

(6) THE DEVELOPMENT OF DRAWING TEXTURES IN COPPER,

(10) R. A. COYLE [redacted] R. B. NETHERCOTT

SUMMARY

An X-ray examination of the development of textures during unidirectional drawing of pure copper at 77K and 196K is reported. Initially, a triplex < 100 >, < 111 >, < 112 > texture is observed in which the < 112 > texture forms rapidly and predominates at low strain. This texture is eventually transformed into a dual < 100 >, < 111 > texture, the rate of transformation being temperature dependent.

Calculations of the X-ray absorption across the cross-section of a wire provide an explanation of observed asymmetries of diffractometer traces and pole figures. Such asymmetries are caused by unidirectional drawing conditions, which favour certain slip directions, creating a partial cylindrical texture.

(11) Jul 77

(12) 28 p.

POSTAL ADDRESS: Chief Superintendent, Aeronautical Research Laboratories,
P.O. Box 4331, Melbourne, Victoria, 3001, Australia.

DOCUMENT CONTROL DATA SHEET

Security classification of this page—Unclassified

1. Document Numbers
   (a) AR Number: AR-000–736
   (b) Document Series and Number: Materials Report 105
   (c) Report Number: ARL/Mat-Report-105

2. Security Classification
   (a) Complete document: Unclassified
   (b) Title in isolation: Unclassified
   (c) Summary in isolation: Unclassified

3. Title: THE DEVELOPMENT OF DRAWING TEXTURES IN COPPER

4. Personal Author(s): R. A. Coyle, R. B. Nethercott

5. Document Date: July, 1977

6. Type of Report and Period Covered:

7. Corporate Author:
   Aeronautical Research Laboratories

8. Reference Numbers
   (a) Task: DST 76/92

9. Cost Code: 34 6720

10. Imprint
    Aeronautical Research Laboratories, Melbourne

11. Computer Program(s)
    ABS—Fortran

12. Document Release Limitations: Approved for Public Release

12-0. Overseas: No.		P.R.	1	A		B		C		D		E	

13. Announcement Limitations (of the information on this page):
    No Limitation

14. Descriptors:
    Anisotropy, Copper, Crystallography, Deformation, Metal drawing, Preferred orientation, X–ray analysis

15. Cosati Codes: 1106 2002

16.

ABSTRACT

An X-ray examination of the development of textures during unidirectional drawing of pure copper at 77K and 196K is reported. Initially, a triplex < 100 >, < 111 >, < 112 > texture is observed in which the < 112 > texture forms rapidly and predominates at low strain. This texture is eventually transformed into a dual < 100 >, < 111 > texture, the rate of transformation being temperature dependent.

Calculations of the X-ray absorption across the cross-section of a wire provide an explanation of observed asymmetries of diffractometer traces and pole figures. Such asymmetries are caused by unidirectional drawing conditions, which favour certain slip directions, creating a partial cylindrical texture.

CONTENTS

1. INTRODUCTION 1

2. THE TRANSMISSION FACTOR FOR X-RAY DIFFRACTION FROM FIBRES 1–2

3. EXPERIMENTAL 2

3.1 Initial Material 2
3.2 Wire Drawing 2
3.3 X-Ray Diffraction 3
3.3.1 Fibre Specimens 3
3.3.2 Pole Figures 3

4. RESULTS 3

4.1 Textures Present 3
4.2 The Intensity Ratio of the < 111 > Texture Arcs 3
4.3 Crystallite Orientation Distribution 3–4

5. DISCUSSION 4

5.1 Interpretation of Diffractometer Traces 4
5.1.1 Textures at Low Strain 4–5
5.1.2 Asymmetry of the < 111 > Texture Arcs 5
5.1.3 Asymmetry of the < 112 > Texture Arcs 5
5.1.4 Symmetry of the < 100 > Texture Arcs 5
5.1.5 Development of Asymmetrical Textures 5–6
5.2 Grain Size and Orientation Distribution 6

6. CONCLUSIONS 6

REFERENCES

FIGURES

DISTRIBUTION

1. INTRODUCTION

In a previous paper (1) on the drawing of pure copper, the development of a dual < 100 >, < 111 > texture was investigated for deformation at temperatures of 293, 373 and 473K. It was found that, when the wire was drawn unidirectionally, the intensities of the < 111 > texture arcs measured on a diffractometer trace taken around the diffraction cone were not the same in the four quadrants. This paper shows that these inequalities arise because (i) the cross-sectional plane normal to the wire axis does not constitute a crystallographic mirror plane, and (ii) the diffracted rays which contribute to the individual arcs have differing path lengths through the specimen. The inequalities can be calculated provided appropriate absorption corrections are applied. Also discussed is the interpretation of the more complex textures formed when copper is unidirectionally drawn at temperatures of 77 and 196K.

Schematic cross-sections of various fibre textures are shown in Fig. 1; the triangles represent the (111) plane faces of octahedrons made up of all the {111} planes viewed from the [111] direction (Fig. 2). The four types represented are (*a*) true fibre, (*b*) single crystal, (*c*) cylindrical and (*d*) and (*e*) partial cylindrical. The first three types have been widely investigated by a number of workers (2, 3, 4, 5, 6, 7); this paper will deal mostly with the partial cylindrical types as found in unidirectionally drawn copper wire. The < 111 > texture has lower symmetry and will be described first; this texture will also be used as a basis for interpreting the diffractometer traces.

A < 111 > fibre texture is defined as having a < 111 > direction oriented parallel to the fibre axis. A true fibre texture is fully defined by this one parameter; the crystallographic directions perpendicular to the fibre axis are randomly oriented (Fig. 1(*a*)). The single crystal fibre texture (Fig. 1(*b*)) consists of a mosaic of crystallites with approximately the same orientation (2) and the cylindrical fibre texture (Fig. 1(*c*)) has a plane, usually the $(11\bar{2})$ in copper, aligned parallel to the fibre surface (8). When there is a spread in the alignment of the $(11\bar{2})$ planes (independent of the spread of the alignment of the < 111 > direction along the axis), the texture is termed partial cylindrical. Two forms of partial cylindrical texture are illustrated in Figs 1(*d*) and (*e*); in the first, there is a random distribution of crystallite misorientation over a limited range with respect to the surface (Fig. 1(*d*)); in the second, the misorientations have a nearest neighbour correlation within the same range of misorientations (Fig. 1(*e*)).

2. THE TRANSMISSION FACTOR FOR X-RAY DIFFRACTION FROM FIBRES

If absorption is negligible and the wire is rapidly rotated (using geometry as in Fig. 3(*a*)), all types of fibre texture give the same X-ray diffraction pattern. In cases where X-ray absorption is appreciable, systematic extinctions and enhancements of the diffraction arcs occur for wires with cylindrical texture (9). Variations of arc intensities, compared with those for a true fibre texture, arise because the diffracting crystallites in the cylindrical texture have different locations, and hence different path lengths, from those in a true fibre texture.

Using a digital computer, the transmission factor for cylindrical X-ray diffraction specimens can be obtained by calculating the path lengths of diffracted rays from all orientations of the diffracting crystallites in all positions in the specimen (10). The program (11) was written using polar co-ordinates with variables r and ω, the origin is at the centre of the wire section and the angular positions of the diffracting crystallites, ω, are measured anti-clockwise from the normal to the diffracting plane (Fig. 4). The transmission factor is found by summing the transmission of each single crystal element $dr.d\omega$. The specimen is spinning about its axis and hence, in the geometry of Fig. 4, all crystallites with diffracting plane normals coplanar with the incident and diffracted beams assume all orientations to the incident X-rays. The angle of incidence of the X-rays will be equal to the Bragg angle for diffraction, θ, only when ω is equal to the

angle between the normal to the diffracting plane and the radius through the centre of the crystallite. Non-equatorial reflections are measured by tilting the specimen through an angle, ϕ, about the axis AB (Fig. 4). The diffracting section of the specimen is thus transformed into an ellipse, thereby providing the general case considered in the program. The calculations for $\omega > 90$ and $\omega < 90$ degrees are done separately to enable computation of path lengths in the interior to be stopped where transmission becomes negligible; this enables a small $dr.d\omega$ to be used with economy of computer time.

Fig. 5 shows the calculated transmission of copper $K\alpha$ X-rays diffracted from 200 planes of copper wire of various diameters. When the diameter is greater than 0·2 mm most of the transmission is from planes which are oriented almost perpendicular to the radius of the wire. Fig. 6 shows the calculated variation of transmission factor with ϕ, the angle of tilt of the specimen, for copper wire of various diameters. The incident beam was assumed to be of uniform height and infinite width, and care was taken to fulfil this condition over the range of ϕ for which the correction was used.

Fig. 7 shows the reflection components which are integrated to make up the transmission factor for the 200 reflection (i.e. $\phi = 35{\cdot}3$ degrees) from a copper wire with a $< 111 >$ true fibre texture. This diagram has been constructed using a stereographic projection (Fig. 8(*a*)) to establish the angles at which particular planes will diffract. The pole of the projection is taken as the $(11\bar{2})$ plane (based on the cylindrical texture for copper (8)); the latitude corresponds to ϕ and the meridian angle to ω. The conditions for maximum transmission, under the conditions of Figs 3 and 4, are met when the pole of a plane is rotated into the pole of projection through angles ϕ and ω.

The crystallites in a true fibre texture have a uniform orientation distribution with respect to ω and hence the average transmission factor can be found by integrating over the range $\omega = \pm 180$ degrees. For a partial cylindrical texture, the transmission factor is found by averaging over the range of ω present and weighting for any non-uniform distribution of crystallites with respect to ω. For a perfect cylindrical texture, the range of ω over which planes may diffract tends to zero for wires of any diameter.

3. EXPERIMENTAL

3.1 Initial Material

High conductivity (oxygen-free), copper rods of 12·7 mm diameter were initially cleaned in a copper bright-dip solution, rotary swaged in 6 steps to 8·7 mm (i.e. approximately 50% reduction in area) and vacuum-annealed at 820K for two hours. After cooling to room temperature, the rod was swaged in 5 steps to 5·7 mm diameter and vacuum-annealed at 820K for two hours. This series of swaging and annealing stages gave a uniform grain size of 30 μm, with a standard deviation of 4, in the 5·7 mm diameter rod. This rod was used as the initial material for wire-drawing. Pole figures taken from longitudinal sections of the rod indicated that the orientations of the grains were nearly random (Fig. 9). This conclusion is consistent with other texture evidence (1) that the initial material was effectively randomly oriented.

3.2 Wire Drawing

The 5·7 mm diameter rod was drawn to various diameters, the smallest of which was 0·18 mm, i.e. strains up to 7 (strain = ln (initial area/final area)). The wire was drawn through the dies in the same direction i.e. no reverse drawing occurred—except in the special case discussed in section 4.2. The drawing speed was 8·7 mm per sec. and the strains per pass were $0{\cdot}25 \pm 0{\cdot}01$ for total strains less than 4·8, $0{\cdot}16 \pm 0{\cdot}02$ for strains from 4·8 to 6·4 and $0{\cdot}25 \pm 0{\cdot}02$ for strains from 6·4 to 7. Colloidal graphite was used as a dry lubricant. The temperatures of drawing were obtained as follows:

(i) Liquid nitrogen (77K),
(ii) Dry-ice (CO_2) in alcohol (196K),
(iii) Room temperature (293K),

3.3 X-Ray Diffraction

3.3.1 Fibre Specimens

X-ray diffraction patterns from single wires were measured using a Stoe four circle goniometer mounted on a Hilger and Watts Y144 powder diffractometer. The incident beam had a divergence of 4 degrees and was 8 mm high, and the receiving slit was adjusted to include all the diffracted beam. Post- and pre-specimen Soller slits with a 1 degree divergence were fitted. The specimen could be rotated about its axis at approximately 2 rotations per second and its diffracting side was aligned on the centre of the incident beam. Copper radiation was used with a proportional counter detector and the counts were recorded on a punched paper tape. The outer surface of the specimen was removed by electropolishing to a depth of either 0·02 mm or 5% of the diameter, whichever was the larger. The polishing solution was made of one part water, two parts orthophosphoric acid and 80 g/l of copper (in the form of cupric phosphate).

3.3.2 Pole Figures

The distribution of crystallite orientations was checked, using pole figures measured from flat specimens, by the Schulz technique (12). Two methods of preparation of the necessary flat specimens are available (13); the first is to remove the interior of the specimen (by spark machining techniques) leaving a thin annulus which is then slit and unrolled, and the second is to mount a number of wires side by side in epoxy resin and to polish them down to a diametral section. The first method is difficult to apply to thin wires and hence the second method was used.

4. RESULTS

4.1 Textures Present

Diffractometer traces of the 200 and 111 diffraction planes of copper wire drawn at 77 and 196K to various strains are shown in Figs 10 and 11. These traces indicate a triplex <100>, <111>, <112> texture. For drawing strains up to 1·7, the textures were poorly developed and it was difficult to assess the relative amounts of each texture present. For these lower strains, the diffraction peaks were sufficiently broad to encompass regions attributable to other textures, in particular the <113> orientation. Indeed, a diffractometer scan of an end section showed the presence of 100, 111, 112 and 113 planes and no indication of 110 planes perpendicular to the wire axis. As deformation proceeded, the diffractometer traces sharpened and more strongly described the <112> orientation until, at a strain of approximately 2·7, the <112> texture had become dominant (Figs 10(*b*) and 11(*b*)). For wires drawn at 196K to higher strains, the amount of the <112> texture then decreased until, at strains above 5·0, it could not be detected and the wire texture was duplex <100>, <111>. It should be noted that, in wires drawn to strains above 1·6 at higher temperatures (viz. 293, 373, and 473K) no trace of a <112> texture was detected (1).

4.2 The Intensity Ratio of the <111> Texture Arcs

An important feature of the traces obtained is their asymmetry about $\phi = 0$, especially for the <111> and <112> components. The intensity ratio for the <111> texture arcs at $\phi = \pm 35{\cdot}3$ degrees on the diffractometer traces from the 200 planes is related to the direction of wire drawing. Fig. 12 shows diffractometer traces from the 200 planes of wires drawn unidirectionally to a strain of 2·4 at 293K and then drawn in the reverse direction to a strain of 4.3. The intensity ratio of the <111> texture arcs varies with the number of passes and the direction of drawing.

A number of copper wires were unidirectionally drawn at temperatures of 196K, and also in previous work at 293, 373, and 473K (1). All wires larger than 0·25 mm diameter had an arc intensity ratio of 0·5, with a standard deviation of 3%.

4.3 Crystallite Orientation Distribution

As shown in previous work (1), wires drawn at a temperature of 293K to strains greater than 1·6 have a dual <100>, <111> preferred orientation along the wire axis. However, the crystallite directions perpendicular to the wire axis are not always randomly distributed

throughout the wire cross-section. This non-randomness is shown by intensity fluctuations in the diffractometer trace of a wire taken at fixed ϕ and θ angles but slowly rotated around the wire axis (Fig. 13(*a*)). This trace was selected as being typical of a specimen exhibiting regions which behave as large mosaic crystals. It should be noted that intensity measurements, referred to in section 4.2, were made on specimens which exhibited minimum fluctuations (Fig. 13(*b*)).

Pole figures may also be used to illustrate non-random crystallite distribution. Pole figures for wires drawn at 293K to strains of 3.1 and 6.1 are shown in Figs 14 and 15. The local peaks in the <100> and <111> texture bands indicate that they have formed into ordered conglomerates.

5. DISCUSSION

5.1 Interpretation of Diffractometer Traces

5.1.1 Textures at Low Strain

As can be seen from Figs 10 and 11, the diffractometer traces do not allow an unambigous determination of the textures present in wires deformed to low strains at 77 and 196K. Fig. 11 shows that, while there are peaks due to the <100>, <111> and <112> textures present, these peaks are broad enough to encompass a range of the textures near to <113>, <114> and <115> orientations. These latter orientations are sufficiently close to <112> that it is likely that they form during initial stages of movement to a <112> orientation. The texture of copper at low strains is thus one in which there is a broad band of fibre axis orientations running between the< 100> and <111> corners of the stereographic triangle with broad local maxima centred on the <100>, <111> and <112> orientations. As strain increases, the peak due to the <112> texture intensifies at the expense of the intensity due to the other local textures and is then itself consumed as <100> and <111> textures become dominant (Fig. 10). Therefore, the most important initial realignment of orientations during deformation is the rotation away from a <110> orientation and this movement occurs before other deformation processes become energetically feasible.

Mechanisms, such as slip and twinning, involved in the formation of deformation textures in f.c.c. metals, have been discussed (14) in terms of Taylor's minimum work criterion (15) for selecting active slip systems. If one assumes that simple {111} <110> slip is most likely to occur during the initial stages of deformation, it is found (16) that crystallite orientations rapidly move away from the <110> orientation towards the band of orientations between <100> and <111> in the stereographic triangle, and eventually towards the <100> and <111> orientations themselves. Thus, at low strains, it is possible for a broad intermediate texture near <112> to form before slipping to the predominant <100> and <111> textures. Other slip processes, such as cross-slip, will accelerate the rate at which movement occurs from <112> to <111>, as well as increasing the final percentage of <111>. Such texture changes are illustrated by the rolling textures of aluminium and silver (17) in which, at low strains (approximately 1), a {110} <112> texture forms, probably as a result of extensive simple slip. Upon further strain, the textures in aluminium and silver diverge in that, at a strain of approximately 3, aluminium has developed a strong {112} <111> texture, presumably by cross-slip, whereas silver remains basically {110} <112>. The increased rate of cross-slip in aluminium is due to its higher stacking fault energy and lower partial dislocation separation, compared with silver.

A definite relationship between rolling and drawing textures is apparent when considering the texture of the flattened outer annulus of a wire and the rolling texture of a sheet of the same metal. It is found that the wire axis corresponds to the sheet rolling direction and the wire radial direction to the sheet normal direction.

An extrapolation of the results of rolled copper (18) to a drawn wire leads one to conclude that, at low strains, wires will have a strong component based on the <112> direction and that this component will gradually transform to the <111> texture during further drawing. The rate at which the transition occurs will depend on the rate of cross-slip, i.e. on both stacking fault energy and temperature. Thus, in the previously reported results on textures in copper at temperatures above 293K (1), which showed only a dual <100>, <111> texture above a

strain of 1.6, the absence of the <112> peaks is due to the higher temperature of deformation assisting the rapid transformation of the initial <112> texture at low strains. It should also be noted from Fig. 11 that the <112> texture has transformed and is not detected at a strain of 5·26 at a deformation temperature of 196K.

5.1.2 Asymmetry of the <111> Texture Arcs

The diffractometer traces from the 200 planes of wires drawn at 77K to a strain of 5·0 and at 196K to a strain of 5·26, show that a duplex <111>, <100> texture is present (Figs 10(*a*), 11(*a*)). However, the <111> texture arc at $\phi = 35{\cdot}3$ degrees has twice the intensity of the arc at —35·3 degrees. From Fig. 7, it can be seen that this condition arises if the (100) and (010) planes contribute to the arc at 35·3 degrees and only the $(00\bar{1})$ plane contributes to the arc at −35·3 degrees. These reflection conditions correspond to a partial cylindrical texture with a uniform distribution of planes over an ω range of ± 90 degrees about the $(11\bar{2})$ plane. This conclusion is confirmed by examining the 111 traces (Figs 10(*b*), 11(*b*)) for strains greater than 5·0); here the <111> texture arc at $\phi = 19{\cdot}5$ degrees is half the intensity of that at −19·5 degrees. This difference in intensity corresponds to the $(11\bar{1})$ plane contributing to the arc at 19·5 degrees, while the $(1\bar{1}\bar{1})$ and $(\bar{1}\bar{1}\bar{1})$ planes contribute to that at −19·5 degrees, as shown in Fig. 8(*a*).

5.1.3 Asymmetry of the <112> Texture Arcs

The complementary $(\bar{1}\bar{1}1)$ [112] and $(11\bar{1})$ [112] stereographic projections (Figs 8(*b*) and 8(*c*)) can be used to show that, for a <112> fibre texture the 200 planes diffract at $\phi = \pm 54{\cdot}7$ and $\pm 24{\cdot}1$ degrees. However, if absorption is appreciable and if the range of distribution of the crystallites is limited to $\omega = \pm 90$ degrees from the $(11\bar{1})$ [112] projection point, then the arcs at −24·1 and 54·7 degrees will not be detected because the path lengths for the 010, $\bar{1}00$ and 001 planes are too long. Conversely, if the crystallites are distributed about the $(\bar{1}\bar{1}1)$ plane, then the arcs at 24·1 and −54·7 degrees will be extinct. This approach is consistent with the presence of arcs at −54·7 and 24·1 degrees and the absence of arcs at 54·7 and −24·1 degrees on the 200 trace of a wire drawn to a strain of 2·6 (Fig. 11(*a*)). Similarly for the 111 trace (Fig. 11(*b*)) where the <112> texture arcs at 70·5, −28·1 and 0 degrees are present and those at −70·5 and 28·1 degrees are not detected.

5.1.4 Symmetry of the <100> Texture Arcs

The intensities of the <100> texture arcs at $\phi = \pm 35{\cdot}3$ degrees on the 111 diffractometer trace (Figs 10(*b*), 11(*b*)) are equal. It can be seen from the (001) [100] projection (Fig. 8(*d*)) that these two <100> texture arcs should be of equal intensity for any distribution of orientation with respect to ω. In all wires examined, the intensities of these two arcs were equal to within a standard deviation of 3%.

5.1.5 Development of Asymmetrical Textures

The ratio of the intensities of the <111> texture arcs at $\phi = \pm 35{\cdot}3$ degrees on the 200 traces (Fig. 11(*a*), strain = 5·26) has been shown to be dependent on the direction of drawing (Fig. 12, para. 4·2) and is therefore a function of deformation conditions.

For homogeneous deformation, the pole figure of a rolled sheet or of a flattened annulus cut from a wire is symmetrical about the deformation and transverse directions, as is found for reverse drawn wire and sheet (19). The presumption that pole figures determined using X-rays are symmetrical is often used to justify the measuring and plotting of one, rather than four, quadrants (20). It has been found, however, that pole figures from unidirectionally deformed sheet are not symmetrical about the transverse direction, (21). In the terminology of Jago and Hatherly (22), the pole figures are double-variant when asymmetrical about the transverse direction (unidirectionally deformed) and four-variant when symmetrical about the transverse and deformation directions.

Asymmetrical textures are likely to be caused by the non-symmetrical forces, present during deformation, activating slip and rotations only in certain directions. These directions will be reversed on either side of the deformation neutral axis (wire axis). The number of crystallite rotations operable during unidirectional deformation will be therefore limited. Thus, a [111] direction which might normally be expected to rotate towards the deformation axis can only do so if the deforming forces activate slip systems which allow it to rotate towards the axis. If

the required slip systems are not activated, another <111> pole may rotate, albeit through a greater angle, towards the axis, and thereby form the texture. Thus, unidirectionally deformed metals examined using low penetration X-rays will exhibit two-variant pole figures from one side of the specimen; when using high penetration neutrons, all the specimen volume is irradiated and a four-variant pole figure results from the addition of the two rotationally twinned, two-variant pole figures from either side of the neutral deformation axis.

With large diameter wires, only those crystallites in the half annulus on the R.H.S. of AB (Fig. 4) have X-ray diffraction path lengths short enough to allow appreciable transmission. When the wire diameter is less than approximately 0·25 mm the crystallites on the L.H.S. of AB can also contribute appreciable intensities to the diffraction arcs, the size of the contribution is shown in Fig. 5. Thus, as can be seen in Fig. 7, for small diameter wires, the intensity due to the (00$\bar{1}$) planes at $\phi = -35{\cdot}3$ degrees is now augmented by the addition of reflections from the ($\bar{1}$00) and (0$\bar{1}$0) planes. Similarly, the (001) planes augment the intensity of the (100) and (010) planes at $\phi = 35{\cdot}3$ degrees. The ratio of the intensity of the arc at 35·3 degrees to that at −35·3 degrees therefore becomes greater than 0·5 for small diameter wires and will approach 1 as the diameter approaches zero.

5.2 Grain Size and Orientation Distribution

Both X-ray diffraction line broadening (23) and electron microscopy (24) show that drawn copper wires have a small crystallite size (about 0·2 to 0·3 μm diameter). If these crystallites have a random distribution of ω angles within a limited range (as in the partial cylindrical case shown in Fig. 1(*d*)) then there should be little variation in the count rate of the diffractometer if θ and ϕ are kept constant and the specimen is slowly rotated around its axis. Such a random distribution of crystallite orientations is not always obtained; some specimens exhibit extreme fluctuations in count rate as the specimen is slowly rotated. An example of this fluctuating count rate is shown in Fig. 13(*a*), for a wire drawn to a strain of 2·4 at 293K.

The fluctuations indicate that the crystallites are not completely random but some short range order of crystallite orientation must be occurring, such as that shown schematically in Fig. 1(*e*). When taking measurements of the relative amounts of <111> and <100> textures present in the wires, care was taken to select specimens which did not show large fluctuations of intensity as the specimen was rotated. It should be noted that the ratio of the intensities of the <111> texture arcs in Fig. 10 is not 0·5 as expected from para 5.1.4; apparently, the condition of uniform crystallite distribution over the range of ω is not met.

6. CONCLUSIONS

Copper wire, drawn at temperatures of 77 and 196K, initially forms a texture based on the <100>, <111> and <112> directions. The <112> based texture forms rapidly and predominates at low strains, but is eventually transformed, and a duplex <100>, <111> texture remains. The rate at which the <112> texture transforms depends on the temperature of deformation, thus accounting for the absence of <112> texture in wires deformed to strains greater than 1·6 at temperatures of 293K and above.

The <111> and <112> texture components possess a partial cylindrical texture, in which the crystallites are oriented in the <111> or <112> directions along the wire axis and also have a tendency to have <112> or <111> directions, respectively, along the wire radius. There is also a limited spread of crystallite orientations about the main orientation, causing the texture to be termed partial cylindrical.

Pole figures resulting from unidirectionally drawn wire and rolled sheet are asymmetrical as a result of certain slip directions being favoured during the deformation process. To obtain symmetrical pole figures, the direction of rolling or drawing must be reversed between passes.

Pole figures represent the average distribution of crystallites over a large volume of specimen and are not necessarily representative of the texture of local regions. Some copper wires possess large volumes in which neighbouring crystallites have similar orientations akin to a mosaic single crystal.

REFERENCES

1. R. B. Nethercott and R. A. Coyle — A.R.L. Report, ARL/Mat. 99, Nov., (1975).
2. W. T. Roberts and R. J. Butt— J. Inst. Metals, **92**, 158–159, (1964–5).
3. G. Linssen, H. D. Mengelberg and H. P. Stuwe — Zeits. Metallkunde, **55**, 600–604, (1964).
4. U. Schlafer and H. J. Bunge — Texture, **1**, 31–49, (1972).
5. H. A. Ahlborn and G. Wassermann — Zeits. Metallkunde, **53**, 422–427, (1962).
6. P. G. Bastien and J. Pokorny — J. Inst. Metals, **82**, 545–549, (1953–4).
7. J. Grewen and G. Wassermann — Zeits. Metallkunde, **45**, 498–505, (1954).
8. H. P. Stuwe — Zeits. Metallkunde, **52**, 34–44, (1961).
9. G. D. Rieck — Philips Res. Rep., **12**, 423–431, (1957).
10. 'International Tables for Crystallography.', **2**, 291, I. U. Cr., (1959).
11. Program ABS available from A.R.L. Computing Centre.
12. L. G. Schulz — J. Appl. Phys., **20**, 1030–1036, (1949).
13. J. Grewen — Zeits. Metallkunde, **61**, 252–260, (1970).
14. G. Y. Chin — 'Textures in Research and Practice' ed. J. Grewen and G. Wassermann, Springer Verlag, pp. 51–80, (1969).
15. G. I. Taylor — J. Inst. Metals, **62**, 307–324, (1938).
16. G. Y. Chin, W. L. Mammel and M. T. Dolan — Trans. Met. Soc. AIME, **239**, 1854–55, (1967).
17. I. L. Dillamore and W. T. Roberts — Acta. Met., **12**, 281, (1964).
18. Hsun Hu, R. S. Cline and S. R. Goodman — 'Recrystallization, Grain Growth and Textures', A.S.M., pp. 295–367, (1966).
19. D. H. Rogers and W. T. Roberts — Zeits. Metallkunde, **65**, 100–105, (1974).
20. W. Bunk — Zeits. Metallkunde, **56**, 645–653, (1965).
21. O. J. Eder and R. Klemencic — J. Appl. Cryst., **8**, 628–635, (1975).
22. R. Jago and M. Hatherly — Metal Science, **9**, 83–89, (1975).
23. R. A. Coyle and R. B. Nethercott, to be published.
24. R. B. Nethercott and J. A. Retchford — A.R.L. Mat. Report, to be published.

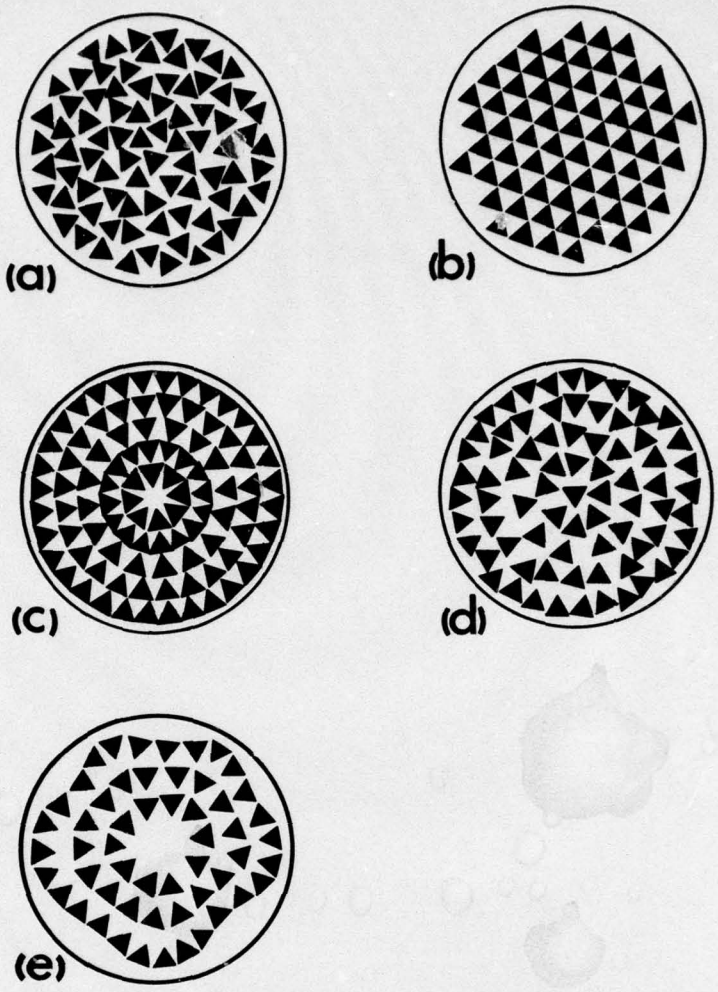

Fig. 1. Cross-sections of 111 wire textures; the crystallites are represented by the triangles formed by the (111) plane faces of the octahedra defined in Fig. 2.
(a) true fibre,
(b) single crystal,
(c) cylindrical,
(d) partial cylindrical,
(e) partial cylindrical.

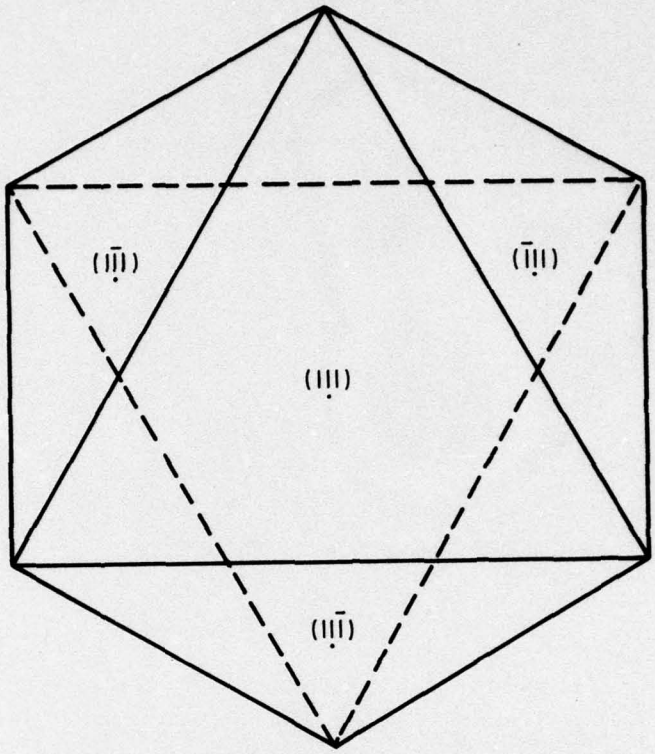

Fig. 2. The octahedron made up of the 111 planes viewed from the [111] direction.

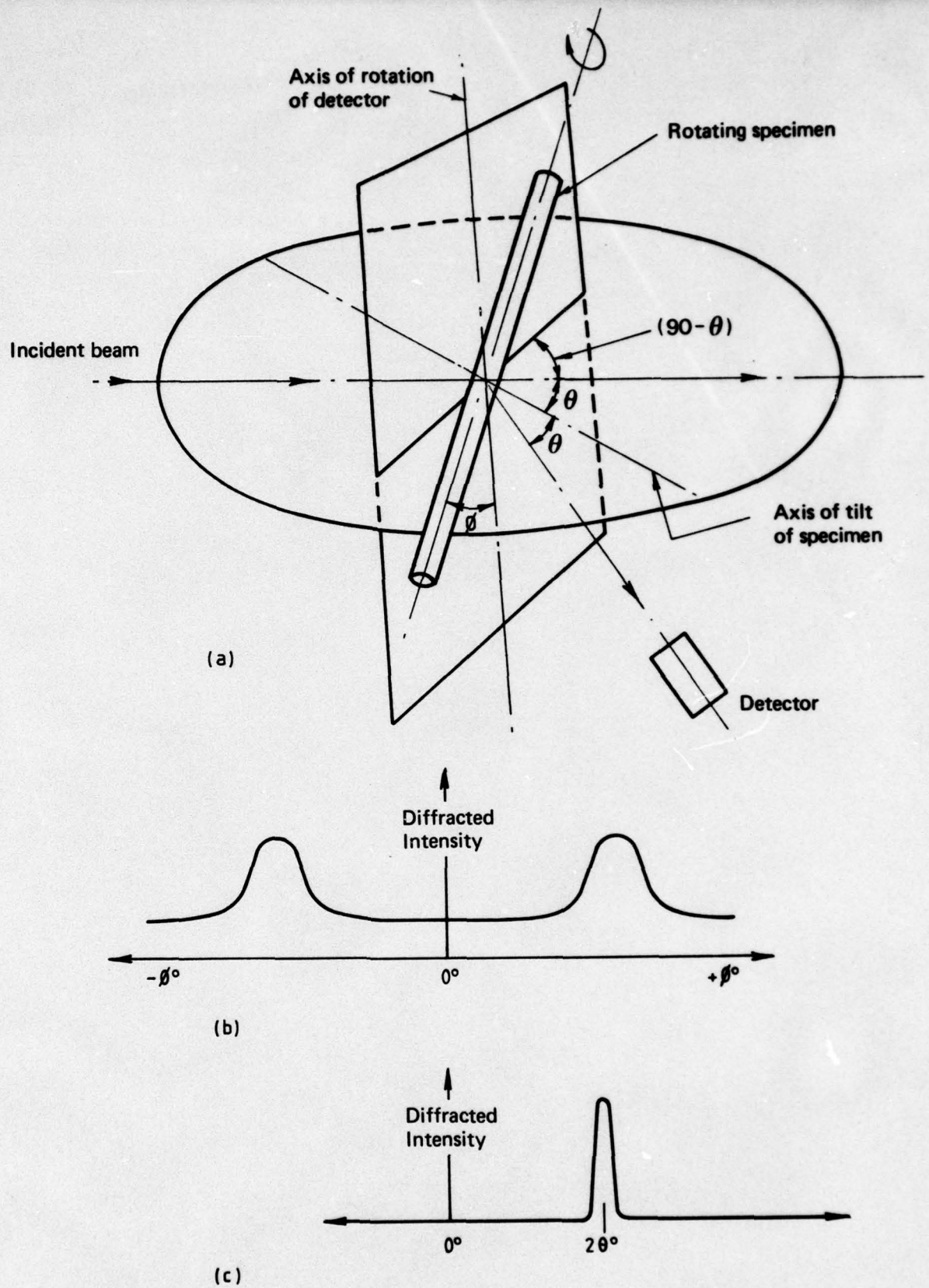

Fig. 3.(a) The X-ray geometry for diffraction from a rotating wire specimen. The axis of tilt and the incident and diffracted rays are coplanar.
(b) The trace of diffracted intensity when the detector is fixed at the angle 2θ and the specimen is moved through the angle ϕ.
(c) The trace of the diffracted intensity when the specimen angle of tilt (ϕ), is fixed and the detector is moved through the angle 2θ.

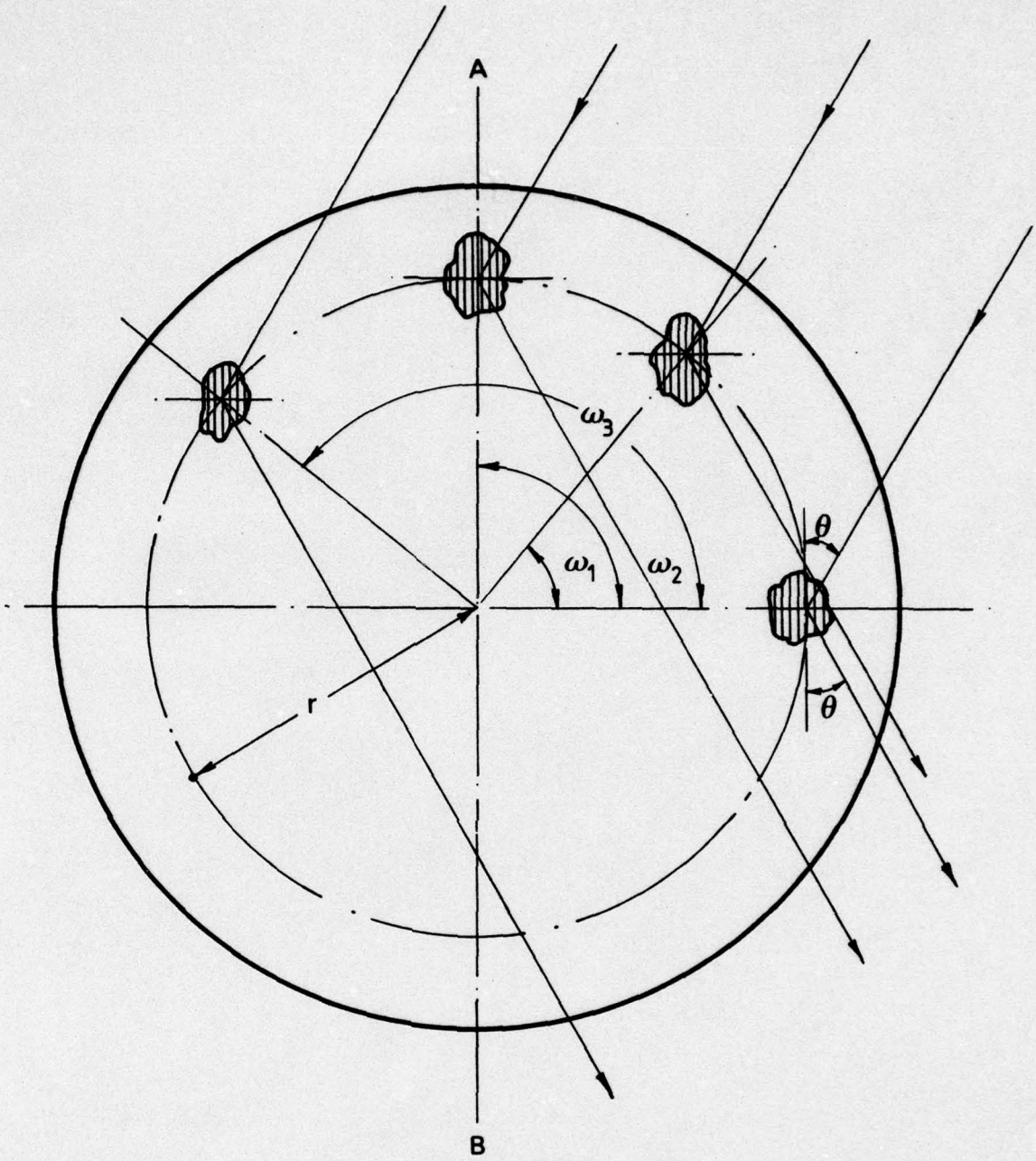

Fig. 4. The paths of rays diffracted from crystallites at a distance r from the wire axis. The diffracting planes are indicated by hatching.

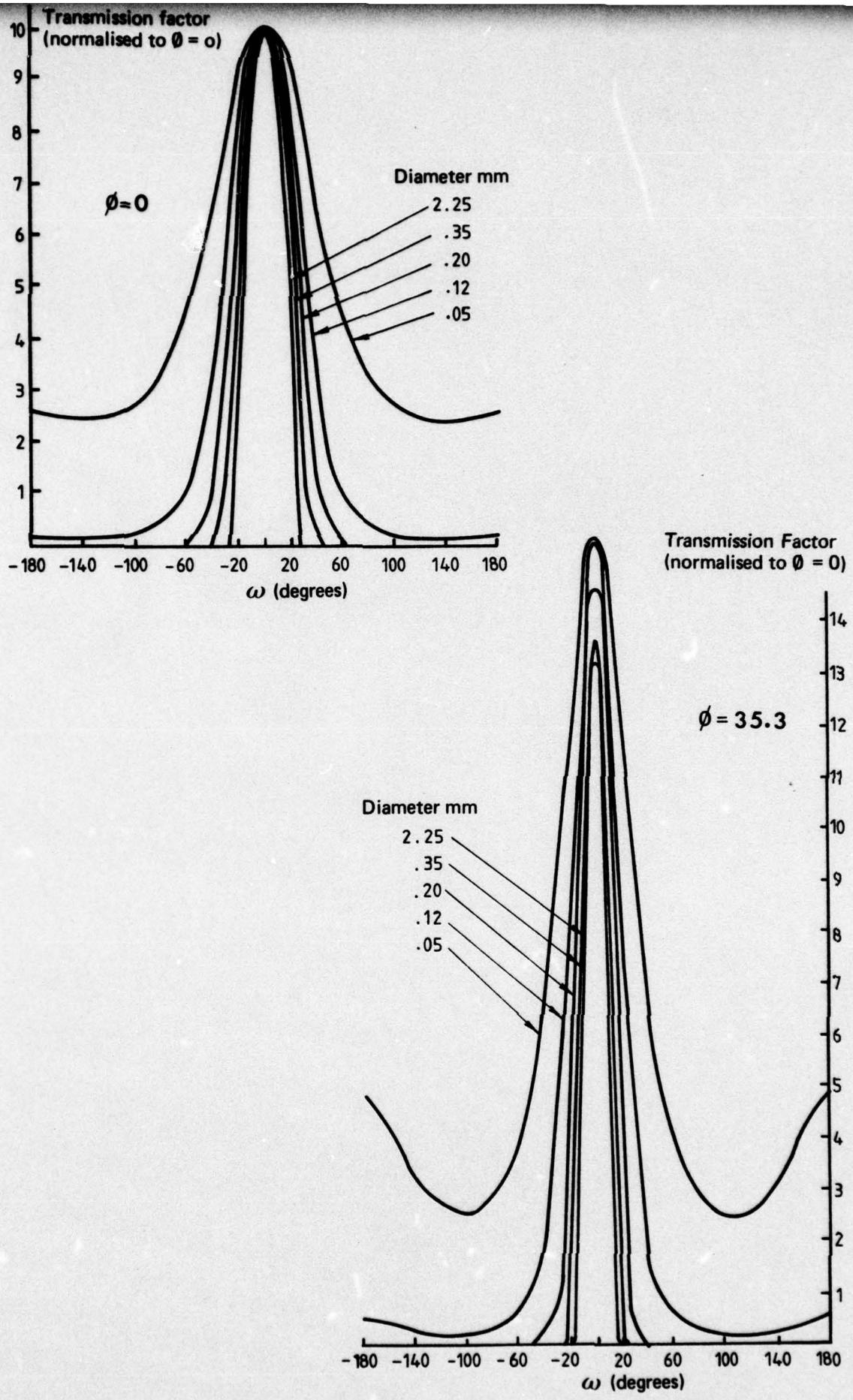

Fig. 5. The calculated transmission of copper Kα X-rays diffracted from the 200 planes in copper wire, as the specimen diameter is varied (a) ϕ=0 (b) ϕ=35.3 degrees. The angle ω is defined in Fig. 4. The transmission is normalized to that at ϕ=0 and 2θ=0.

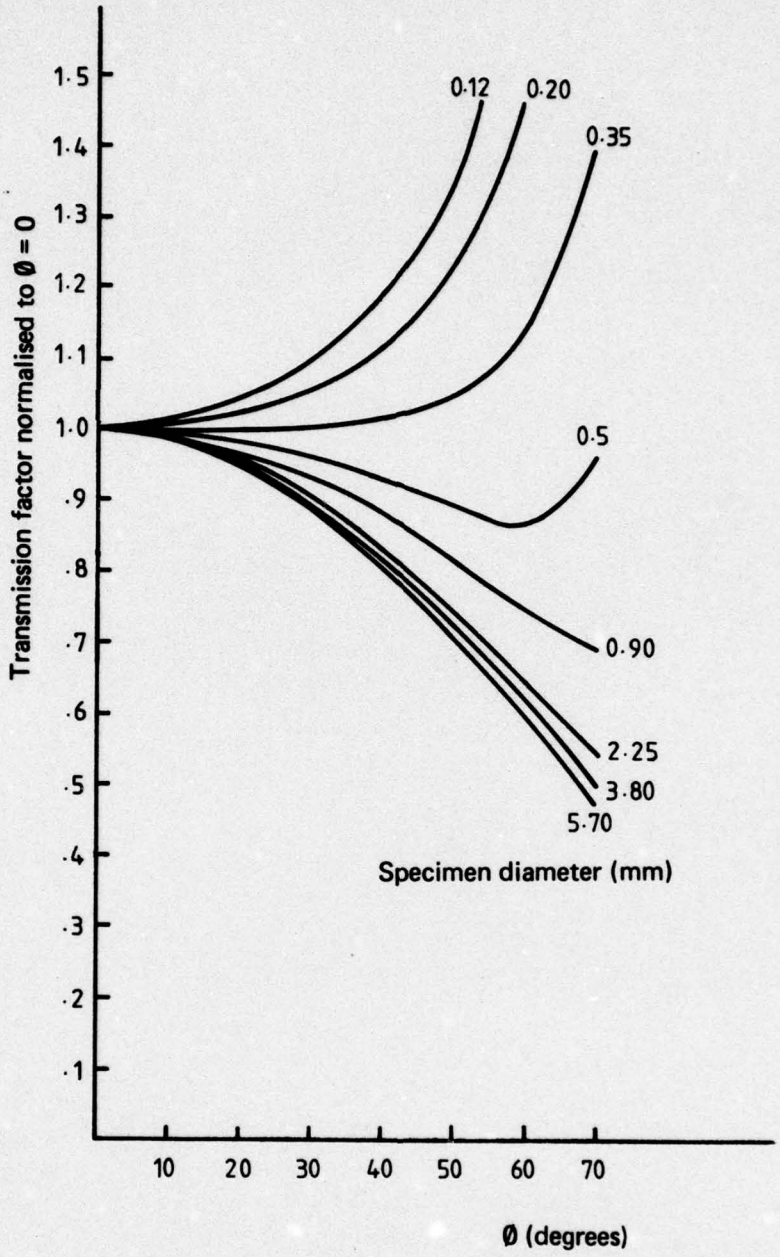

Fig. 6. The calculated transmission for copper Kα X-rays from the 200 planes of copper wire, for various wire diameters, as the specimen is tilted through an angle ϕ. The calculated transmission factor is normalized to that at ϕ=0.

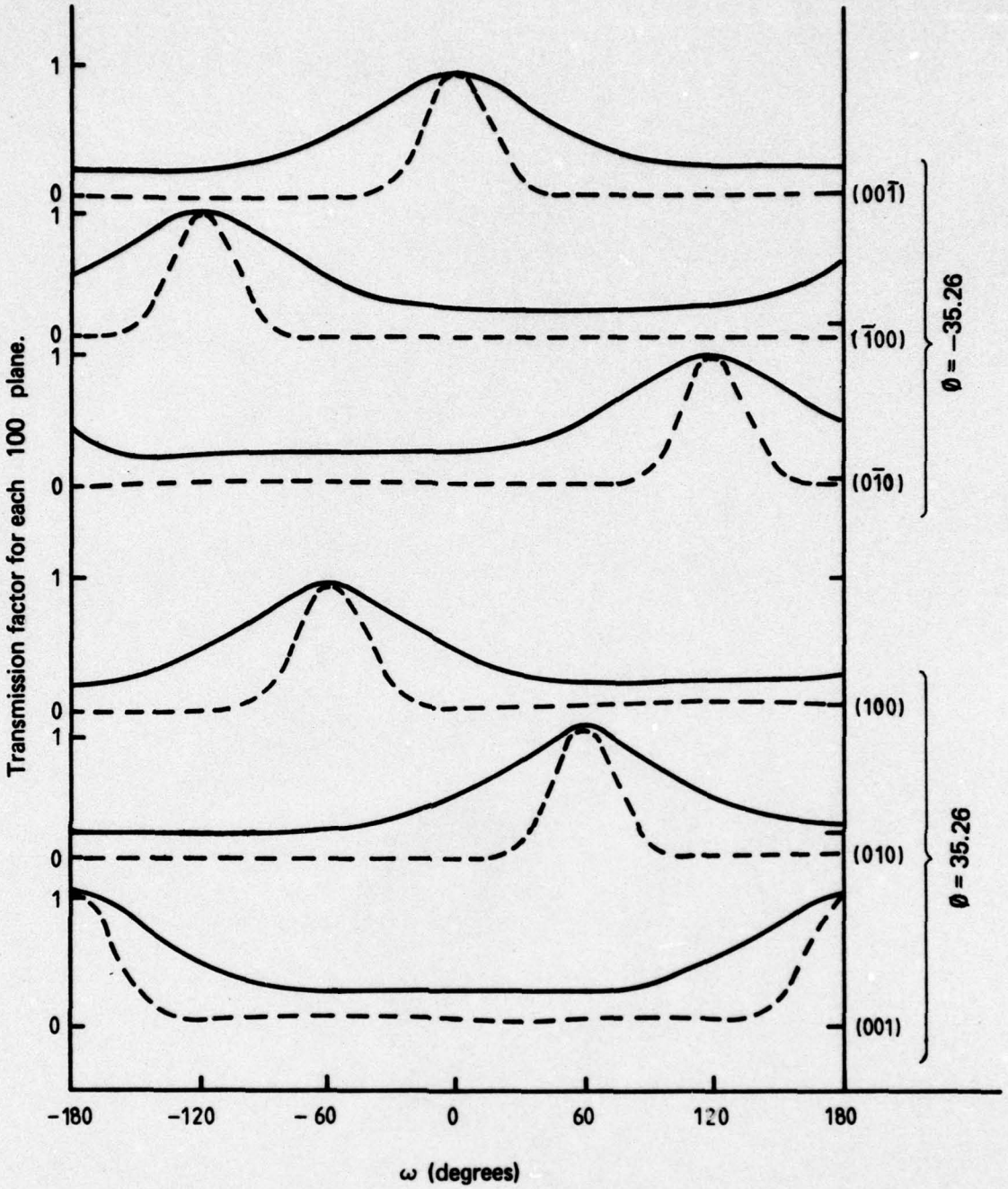

Fig. 7. The transmission factor for copper Kα X-rays diffracted from each 100 plane as the crystallite is rotated through an angle ω. (a)– – –wire diameter 0.35 mm (b)—— wire diameter 0.05 mm.

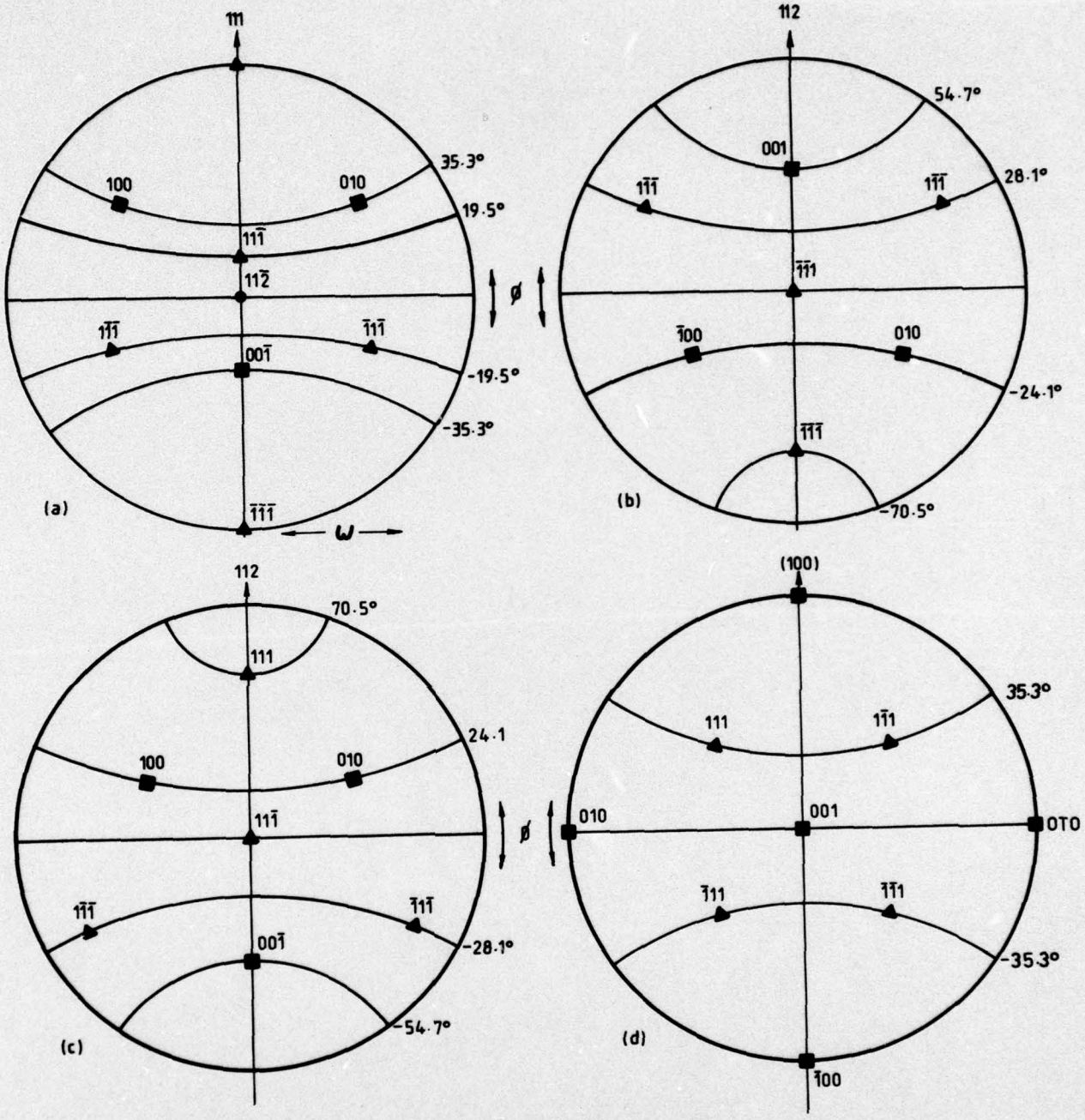

Fig. 8. Stereographic projections for cubic cell;
(a) (11$\bar{2}$)[111]
(b) ($\bar{1}\bar{1}$1)[112]
(c) (11$\bar{1}$)[112]
(d) (001)[100]

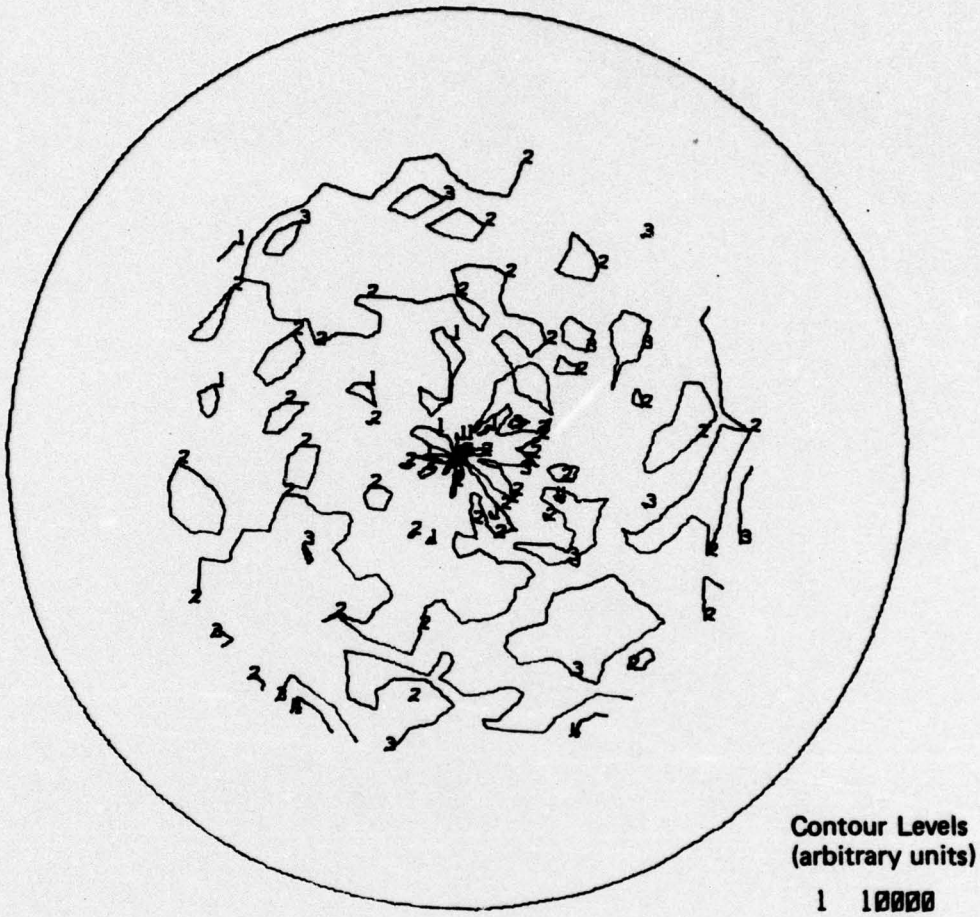

Contour Levels
(arbitrary units)

1	10000
2	20000
3	30000
4	40000

Fig. 9. The 111 pole figure of equiaxed copper rod prior to drawing.

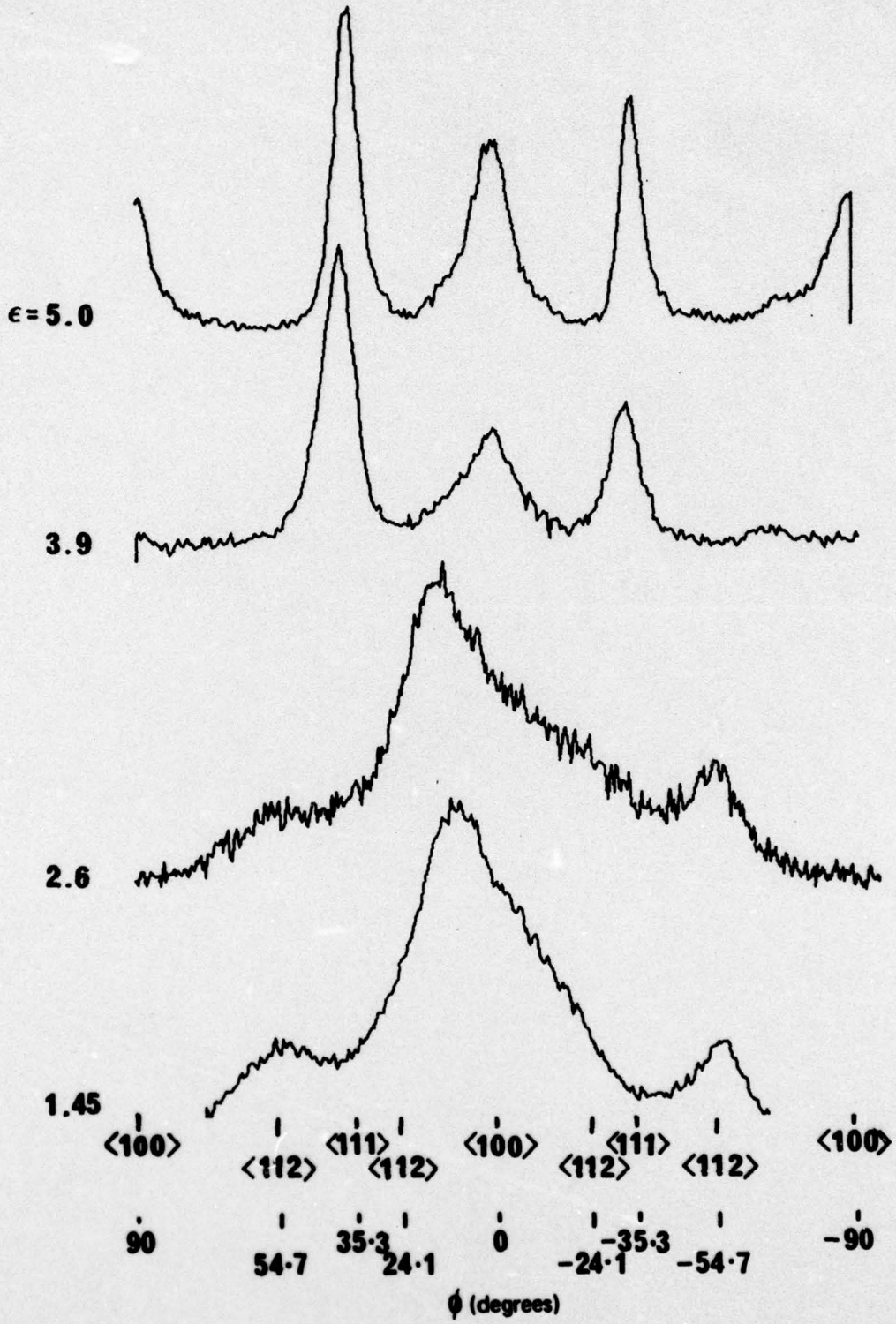

Fig. 10(a). Diffractometer traces of the angular distribution of intensity from the 200 planes of wires drawn at 77K to strains as shown.

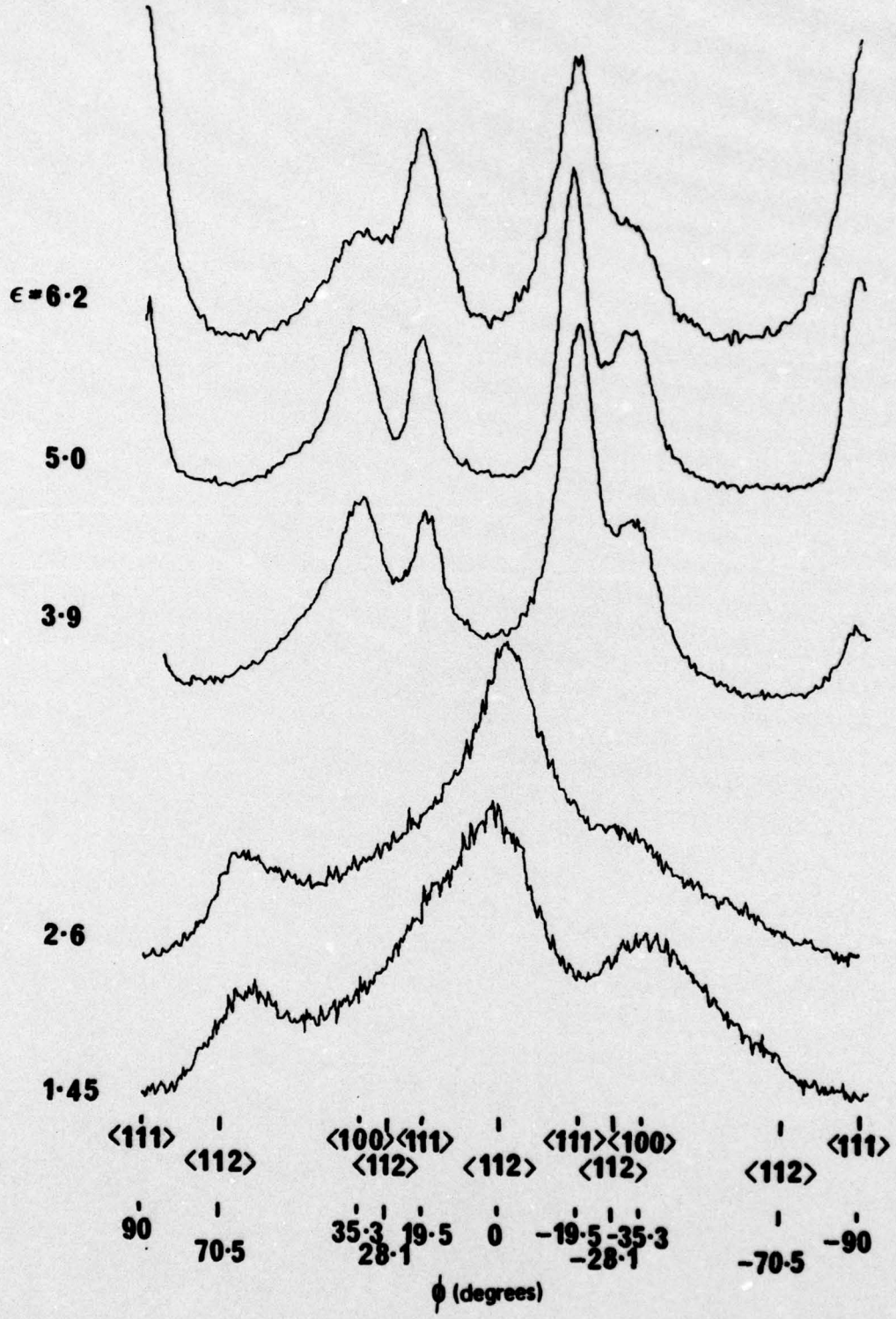

Fig. 10(b). Diffractometer traces of the angular distribution of intensity from the 111 planes of wires drawn at 77K to strains as shown.

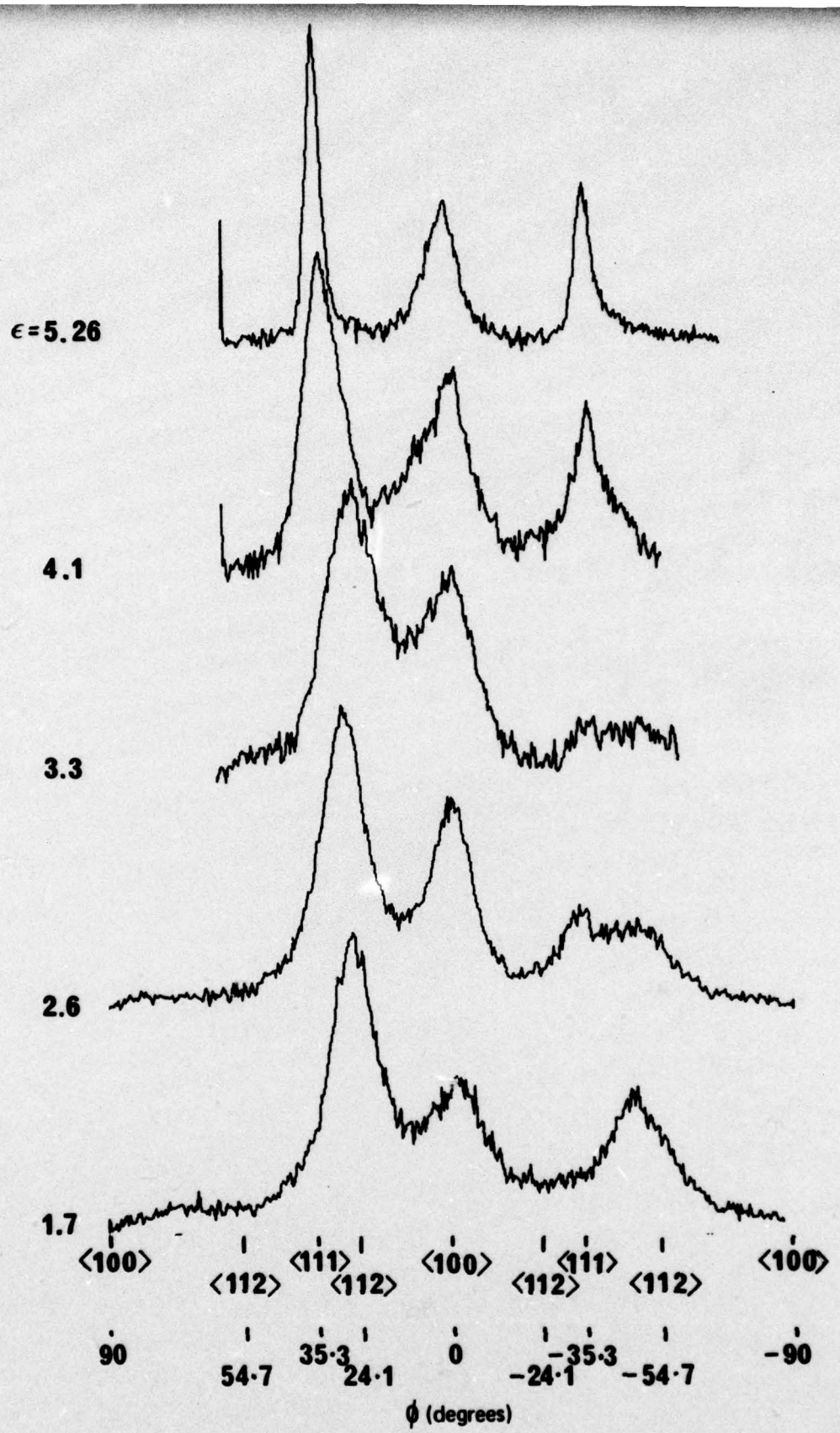

Fig. 11(a). Diffractometer traces of the angular distribution of intensity from the 200 planes of wires drawn at 196K to strains as shown.

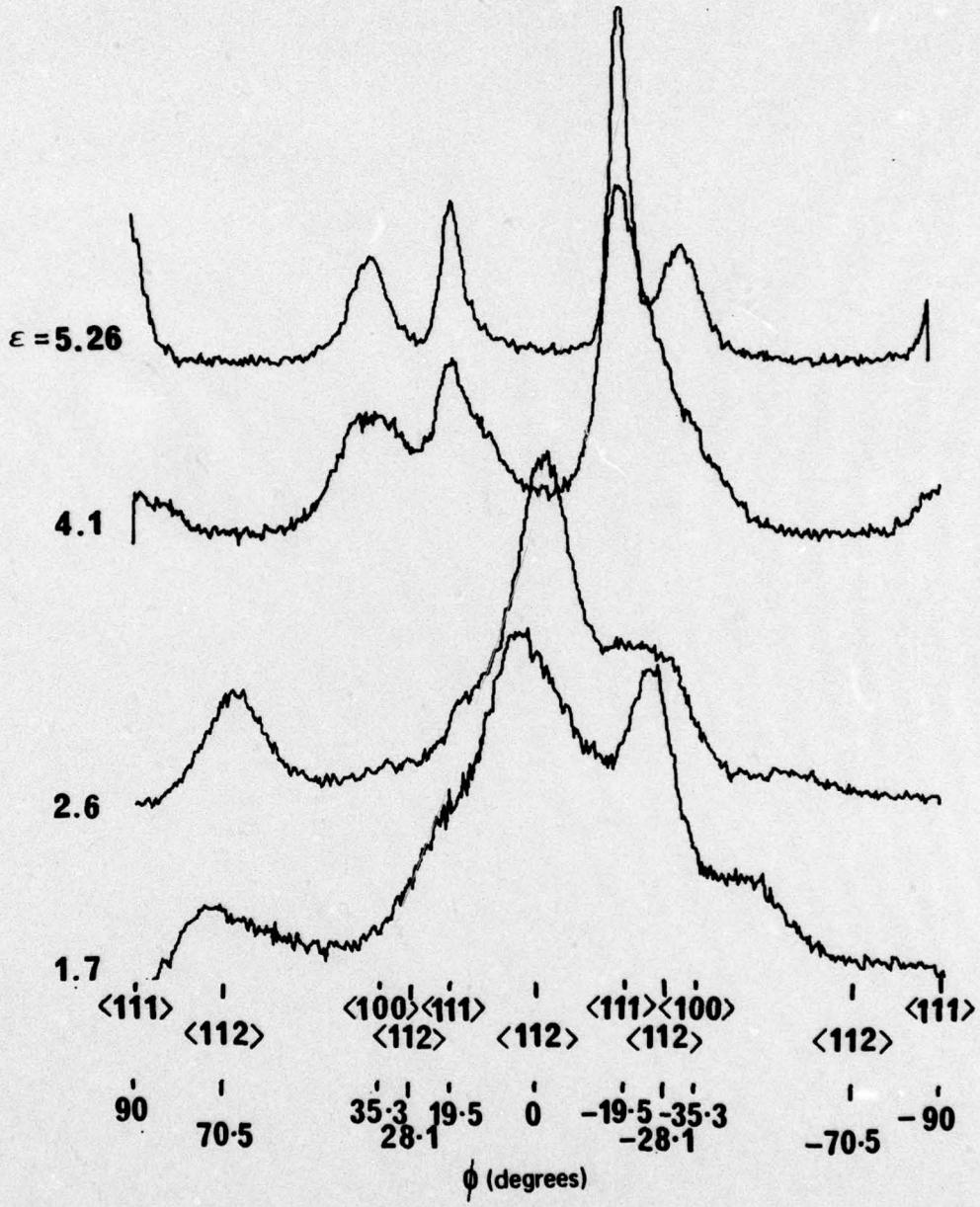

Fig. 11(b). Diffractometer traces of the angular distribution of intensity from the 111 planes of wires drawn at196K to strains as shown.

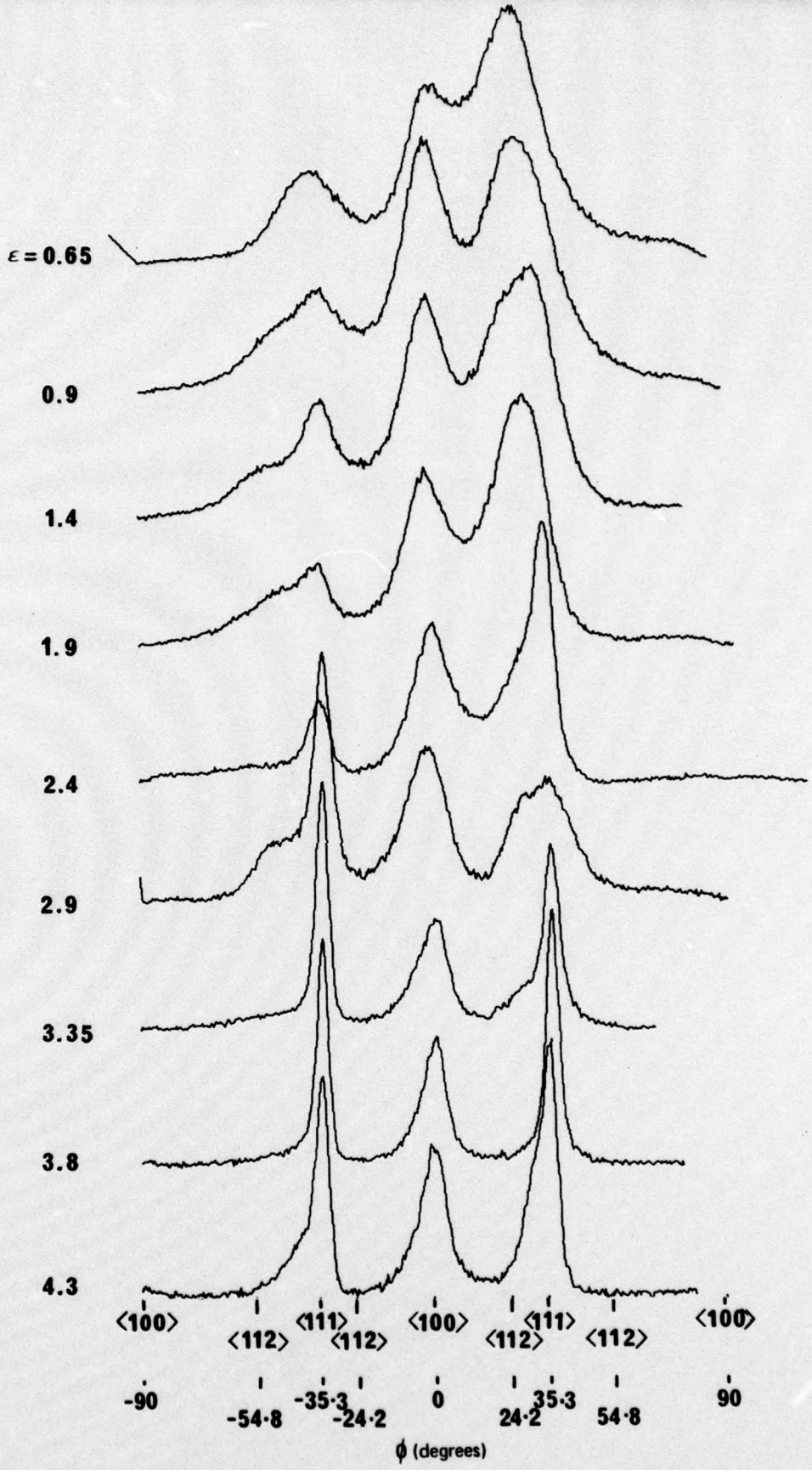

Fig. 12. Diffractometer traces of the intensity from the 200 planes of a wire drawn unidirectionally at 293K to a strain of 2.4 and then in the opposite direction to a strain of 4.3.

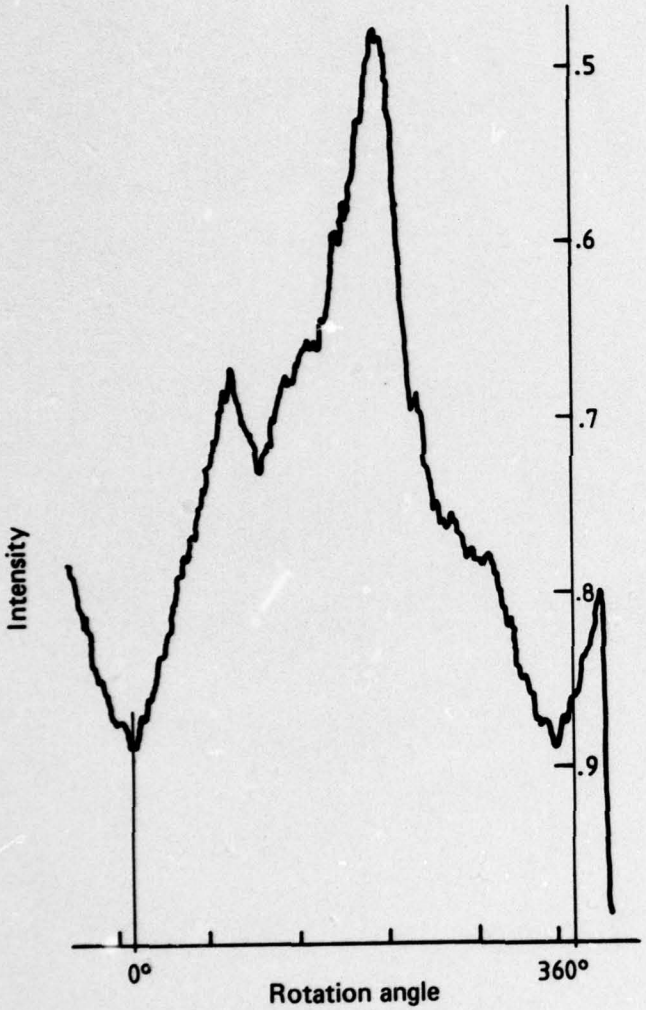

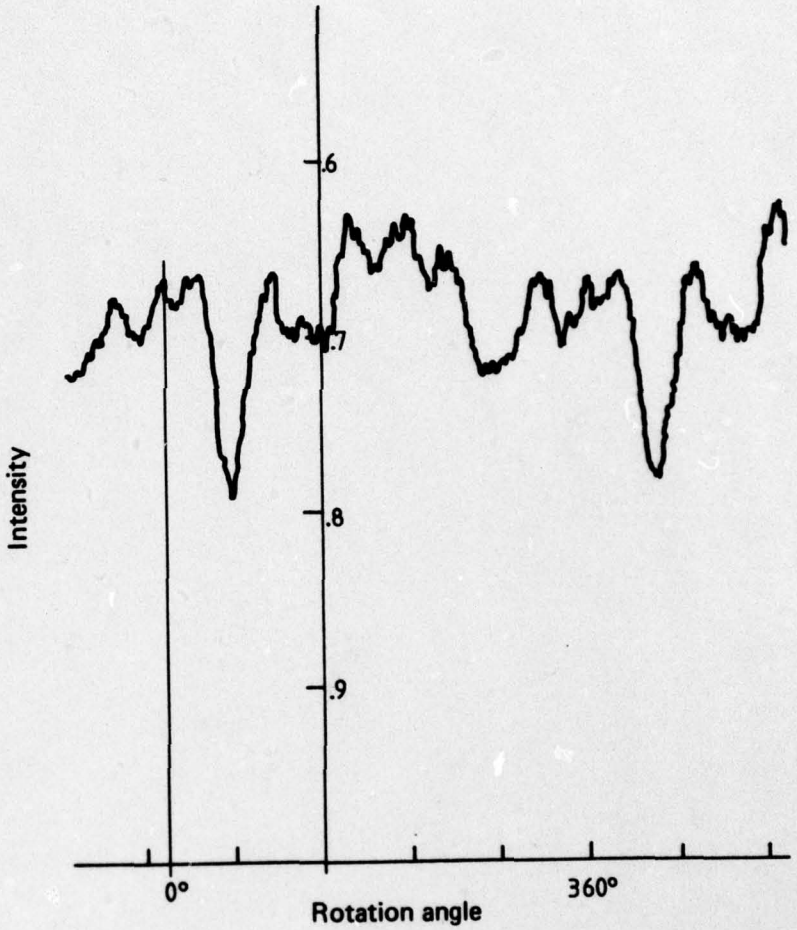

(a) (b)

Fig.13. The diffracted intensity taken at fixed θ and ϕ with the specimen slowly rotating about its axis. Wire drawn at 293K to a strain of 3.6.
(a) specimen exhibiting large mosaic crystallite size,
(b) specimen exhibiting small mosaic crystallite size.

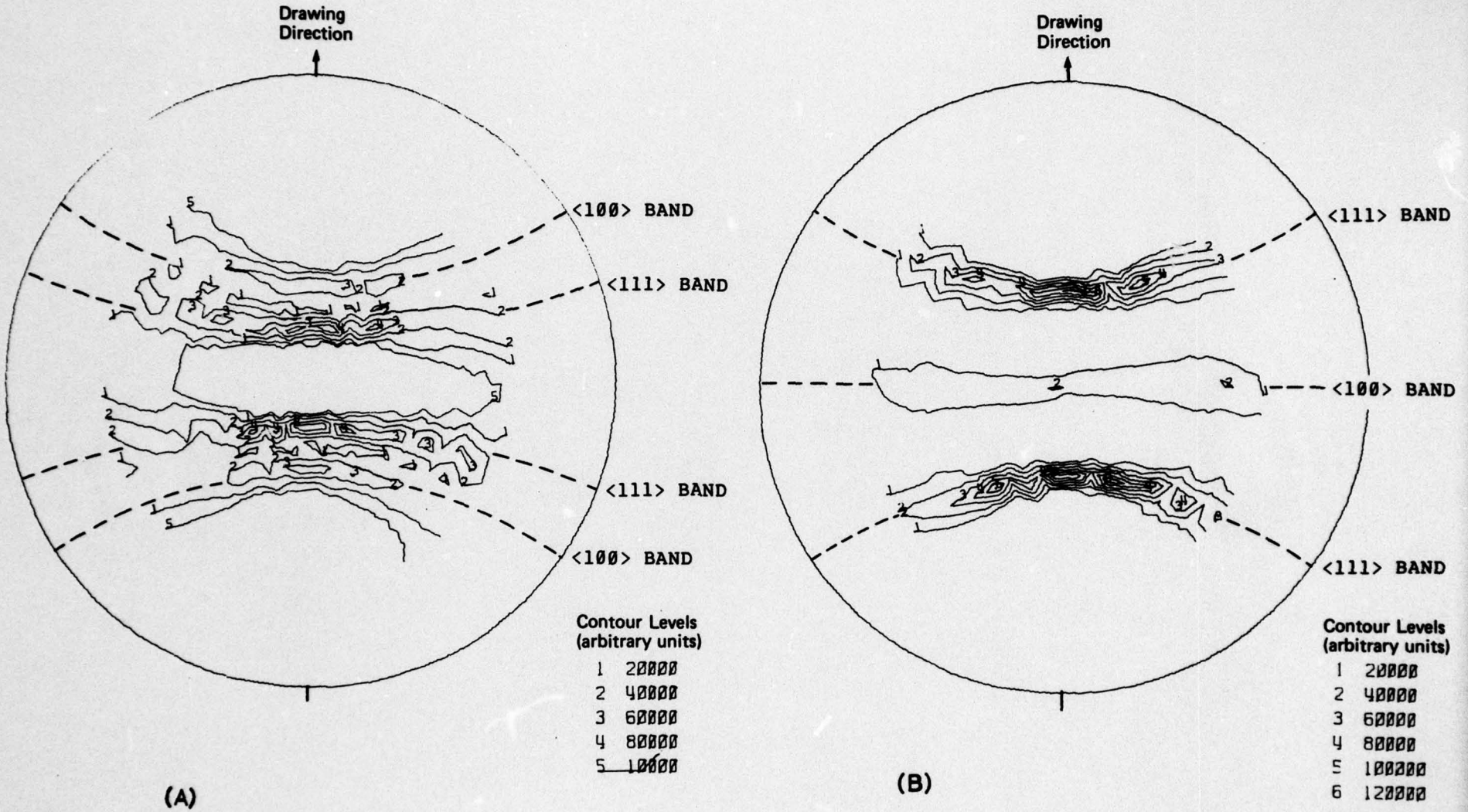

Fig. 14. Pole figures of copper wire drawn at 293 K to a strain of 3.1.

(a) 111 planes
(b) 200 planes

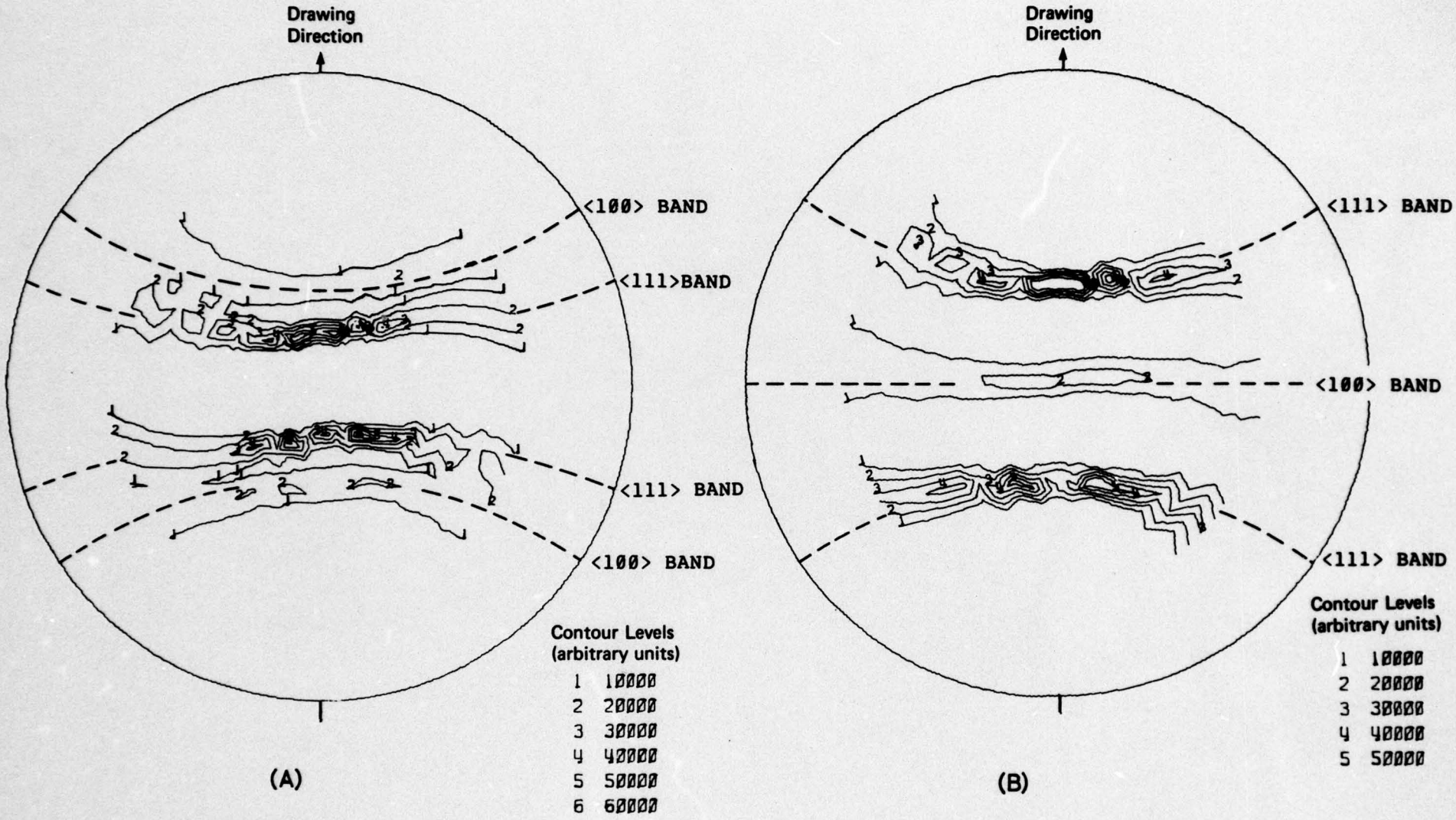

Fig. 15. Pole figures of copper wire drawn at 293K to a strain of 6.1.
(a) 111 planes
(b) 200 planes

DISTRIBUTION

Copy No.

AUSTRALIA

DEPARTMENT OF DEFENCE

Central Office

Chief Defence Scientist	1
Executive Controller, ADSS	2
Superintendent, Defence Science Administration	3
Defence Library	4
J.I.O.	5
Assistant Secretary, DISB	6–23

Aeronautical Research Laboratories

Chief Superintendent	24
Superintendent — Materials	25
Divisional File — Materials	26
Authors — R. A. Coyle	27
R. B. Nethercott	28
Library	29

Materials Research Laboratories

Library	30

Weapons Research Laboratories

Library	31

Engineering Development Establishment

Library	32

RAN Research Laboratory

Library	33

STATUTORY, STATE AUTHORITIES AND INDUSTRY

Australian Atomic Energy Commission (Director) N.S.W.	34
C.S.I.R.O., Central Library	35
C.S.I.R.O., National Measurement Laboratory (Chief)	36
C.S.I.R.O., Tribophysics Division (Director)	37
Gas and Fuel Corporation (Research Director)	38
S.E.C. Herman Research Laboratory (librarian) Victoria	39
S.E.C. of Queensland, Library	40
BHP Central Research Laboratories, N.S.W.	41
BHP Melbourne Research Laboratories	42
Comalco Research Laboratories (Dr. J. Eady)	43
Conzinc Riotinto of Australia (Dr. Worner) Victoria	44

UNIVERSITIES AND COLLEGES

Adelaide	Barr Smith Library	45
Australian National	Library	46
Flinders	Library	47
James Cook	Library	48
La Trobe	Library	49
Melbourne	Engineering Library	50
Monash	Library	51
	Professor I. J. Polmear, Materials Engineering	52
Newcastle	Library	53
New England	Library	54
New South Wales	Physical Sciences Library	55
	Prof. M. Hatherly	56
Queensland	Library	57
Sydney	Library	58
Tasmania	Engineering Library	59
Western Australia	Library	60
RMIT	Library	61

AUSTRIA

Dr. Otto J. Eder, Forshungszentrum Seibersdorf 62

CANADA

Aluminium Laboratories Ltd, Library 63
Energy, Mines and Resources Department, Physics and Metallurgy:
Research Laboratories (Dr A. Williams) 64
NRC, National Aeronautics Establishment, Library 65

UNIVERSITIES

McGill Library 66
Sir George Williams University (Prof. H. J. McQueen) 67

FRANCE

AGARD, Library 68
Institute Francais de Petrole, Library 69
ONERA, Library 70
Service de Documentation, Technique de l'Aeronautique 71

GERMANY

Dr. K. Lucke, Technische Hochschule, Aachen 72
ZLDI 73
Dr. H. Bunge, Technische Universitat, Clausthal 74

INDIA

CAARC Co-ordinator Materials 75
Indian Institute of Science, Library 76
Indian Institute of Technology, Library 77

JAPAN

National Aerospace Laboratory, Library 78

UNIVERSITIES

Tohuku (Sendai) Library 79

NETHERLANDS

Central Organization for Applied Science Research in the Netherlands TNO, Library 80
National Aerospace Laboratory (NLR), Library 81

NEW ZEALAND

UNIVERSITIES

Canterbury Library 82

SWEDEN

Kungl. Tekniska Hogscholens 83

UNITED KINGDOM

Australian Defence Science and Technical Representative 84
Aeronautical Research Council, N.P.L. (Secretary) 85
C.A.A.R.C. N.P.L. (Secretary) 86
Royal Aircraft Establishment Library, Farnborough 87
Royal Aircraft Establishment Library, Bedford 88
Admiralty Materials Laboratories (Dr. R. G. Watson) 89
British Library, Science Reference Library 90
British Library, Lending Division 91
Aircraft Research Association, Library 92
British Non-Ferrous Metals Association 93
British Steel Corporation. Corporate Development Lab. (Dr. I. L. Dillamore) 94
Central Electricity Generating Board 95
Fulmer Research Institute Ltd (Research Director) 96
Metals Abstracts (Editor) 97
Science Museum Library 98

UNIVERSITIES AND COLLEGES

Bristol	Library, Engineering Department	99
Birmingham	Dr. W. T. Roberts	100
	Prof. R. E. Smallman	101
	Dr. W. B. Hutchinson	102
Cambridge	Library, Engineering Department,	103
	Dr. G. J. Davies	104
Leeds	Professor J. Nutting	105
Nottingham	Library	106
Oxford	Dr. P. M. Hazzledine	107
Sheffield	Dr. C. M. Sellars	108
Southampton	Library	109
Strathclyde	Library	100
Sussex	Prof. R. W. Cahn	111
Cranfield Institute of Technology	Library	112
Imperial College	The Head	113

UNITED STATES OF AMERICA

Counsellor, Defence Science	114
N.A.S.A. Scientific and Technical Information Facility	115
ARMCO Steel Corp (Dr. P. Morris)	116
Applied Mechanics Reviews	117
The Chemical Abstracts Service	118
Spares	119–128